JOURNAL OF QUATERNARY SCIENCE (2024) **39**(6) 972–986 ISSN 0267-8179. DOI: 10.1002/jqs.3646

JQS Journal of Quaternary Science QRA Quaternary Research Association

Holocene climate evolution and human activity as recorded by the sediment record of lake Diss Mere, England

LAURA BOYALL,[1]* CELIA MARTIN-PUERTAS,[1] RIK TJALLINGII,[2] ALICE M. MILNER[1] and SIMON P. E. BLOCKLEY[1]
[1]Department of Geography, Royal Holloway University, Egham, UK
[2]GFZ-German Research Centre for Geosciences, Potsdam, Germany

Received 10 October 2023; Revised 26 June 2024; Accepted 27 June 2024

ABSTRACT: Lake sediments are ideal archives to evaluate the interactions between climatically driven environmental responses and human activity on seasonal to multi-decadal timescales. This study focuses on the unique sediments of Diss Mere, the only lake in England providing an annually laminated (varved) record for most of the Holocene. We combine microfacies analysis with X-ray core scanning data to explore the influence of natural and human-led changes on sediment deposition over the past 10 200 years and evaluate the sensitivity of the lake sediments to climate variability through time. Variability of titanium (Ti), calcium (Ca) and silica (Si) explain most of the lithological changes observed in the sediment and we identify three stages with low (10 290–2070 cal a BP), intermediate (2070–1040 cal a BP) and intensified (1040 cal a BP – present) human influence. During the first stage, where varved sediments are preserved, Ti is low due to the minimal detrital input into the lake. Ca and Si during this stage reveal high-amplitude variability responding to seasonal changes in sediment deposition. The termination of varved sediment preservation and increases in sedimentation rates coincide with a major rise in Ti after this first stage, marking the intensification of human activity around the lake. Ca is used here as an indicator of temperature-included calcite precipitation, and the long-term variability of the Ca profile resembles Holocene temperature evolution. This continues during periods of intensified human activity, suggesting that the Diss Mere sediments remain sensitive to climate through time. © 2024 The Authors. *Journal of Quaternary Science* Published by John Wiley & Sons Ltd.

KEYWORDS: climate; human land use change; varved lake sediments; XRF core scanning

Introduction

Lake sediments as environmental archives

Lake sediments are used frequently in palaeoenvironmental and palaeoclimatic reconstructions due to their ability to rapidly respond to changing external conditions (Cohen, 2003). Some lakes preserve sediment sequences that are annually laminated (varved) (Zolitschka et al., 2015), which record variability on a range of timescales from seasonal and annual, to centennial and multi-millennial. Alterations in the biological, chemical and physical processes of lakes and their catchments can be driven by both human activity and climate variability (Olsen et al., 2010; Żarczyński et al., 2019). These changes can cause distinct signatures in the deposition of sediment and subsequently its geochemical composition and have been used to reconstruct the pace and impact of external drivers on lake systems through time. A wide range of techniques are used to interpret lake sediments and their associated forcing variables including: microfacies analysis (Brauer et al., 2008; Dräger et al., 2017); palaeoecological proxies such as pollen, diatoms and macrofossils (e.g. Harding et al., 2022; Müller et al., 2021); stable isotope analyses (e.g. Jonsson et al., 2010); and X-ray fluorescence (XRF) core scanning (e.g. Czymzik et al., 2023; Makri et al., 2020; Zander et al., 2021; Martin-Puertas et al., 2017).

Non-destructive and near-continuous analyses using XRF core scanning data can accurately track changes in the geochemical composition of sediment (Kern et al., 2019). When combined with well-refined chronologies, XRF element records enable reconstructions of different processes on timescales which are relevant to human lifetimes (Dräger et al., 2017). Records of chemical elements, or element ratios, have been used as geochemical proxies to track depositional changes associated with both internal lake variability (e.g. lake mixing or stratification) and external drivers (e.g. temperature, precipitation, human activity). However, the limited number of major and minor geochemical elements obtained from bulk sediment analyses can strongly differ due to different site-specific features including lake morphometry and catchment geology (Davies et al., 2015). Additionally, the link between depositional changes and environmental and/or climate variability is not straightforward. As a result, it is common practice to complement the XRF core scanning data with additional proxies through a multiproxy approach such as microfacies analysis, pollen and hyperspectral imaging, to ensure that informed interpretations are made (Martin-Puertas et al., 2017; Peti and Augustinus, 2022; Zander et al., 2021).

The Holocene is the only interglacial period where the interactions between natural climate variability and past human activity can be properly assessed. Significant changes in land use began with the switch between different historic cultural groups, such as shifts from hunter-gatherers to agrarian societies in the Mid-Holocene (Warden et al., 2017), and intensification in human activity from the Late Iron Age and Roman periods (Jones et al., 2022). Human activity within a lake catchment adds to the complexity of interpreting proxy signals recorded in lake sediments, posing several palaeolimnological challenges. To investigate these challenges we address the following

*Correspondence: Laura Boyall, as above.
E-mail: laura.boyall.2016@live.rhul.ac.uk

questions: (i) what implications does changing land use have on lake functioning? (ii) How does changing land use effect sediment deposition and preservation? And finally, (iii) are the geochemical proxy data sensitive to climate variability despite human activity present in the catchment? We address these questions using the Holocene lake sediments of Diss Mere, a small urban lake in the UK. The current lake and sediment record is well studied and reveals a clear sensitivity to natural climate and environmental variability, as well as human land use change (Peglar, 1993; Peglar et al., 1984; Martin-Puertas et al., 2023; Boyall et al., 2023). In addition, it is currently the only published lake record in the UK with a continuous varved sequence through much of the Holocene. The Holocene varves extend from 10 290 to 2069 years before present (before 1950 CE, cal a BP hereafter; Martin-Puertas et al., 2021). Combining microfacies analysis and XRF core scanning data allows us to explore sedimentological and compositional variations on seasonal to annual timescales. Linking these variations with Holocene climate variability and human activity around the lake can then help identify whether the intensification of human activities through history affected how climate variability was recorded in the lake sediments and the proxies they hold.

Study site and human occupation

Diss Mere (52°22′N, 1°6′E, 29 m a.s.l.) is situated in the town of Diss, England (Fig. 1). The current lake system has a maximum water depth of 6 m (Fig. 1b), and a surface area of 0.034 km^2 and is a marl lake system with alkaline waters (Boyall et al., 2023). The hydrological catchment has an approximate area of 1.5 km^2 and is situated within the Waveney Valley (Fig. 1c). Groundwater entering the lake is minimal (Boyall et al., 2023). The regional climate follows a seasonal pattern with mean maximum air temperatures in July (17.4°C), and minimum temperatures in January (4.4°C). Being on the eastern side of the UK, rainfall is much less than for other regions of the UK (Mayes, 2000), with a mean annual total of ca. 630 mm.

Diss is recognized as a historic town with a long history of a market trade industry since the Medieval period (Peglar, 1993; Pursehouse, 1961). However, as reconstructed through palynological data from previous Diss Mere studies, the lake catchment experienced a longer history of human settlement (Peglar, 1993). Palynological analysis suggested that during the Mid-Holocene, human activity remained low with only isolated changes to the vegetation through the Neolithic period. The first substantial changes were recorded during the Iron Ages (800 BCE – 43 CE, Needham, 2007), where significant forest clearances occurred and the vegetation was replaced by arable crops and farmland (Peglar, 1993). In the Anglo-Saxon period (400–1066 CE, Reynolds, 1985), rising population numbers for Diss and surrounding towns coincided with the further development of the landscape, and more arable crops were planted to support this population growth. The modern town of Diss was established during the Medieval period, when Diss became a leading centre for the fabric trade, focusing mostly on wool and linen, but subsequently expanding to both the cultivation and trading of hemp (*Cannabis sativa*), most notably between the 15th and 17th centuries (Blomfield, 1805,

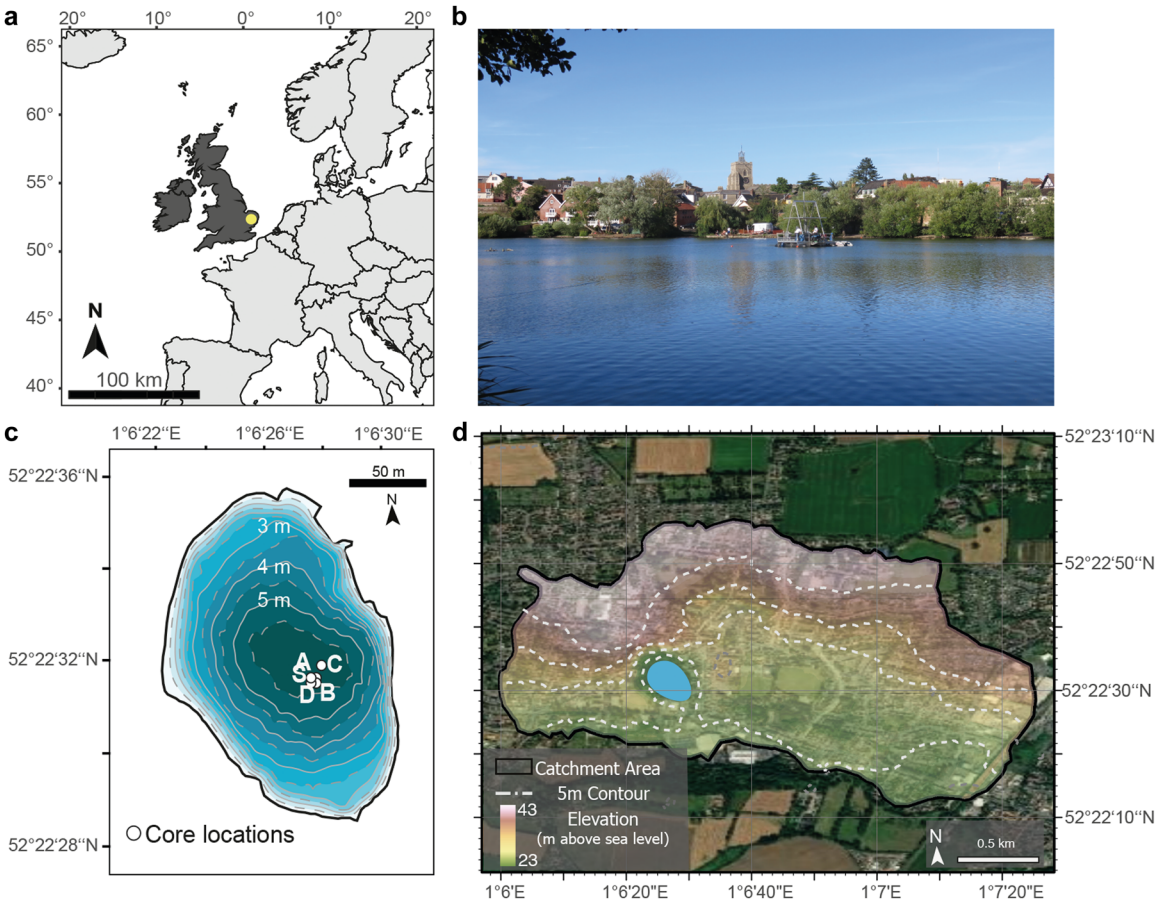

Figure 1. Location maps of the Diss Mere study site. (a) Regional map of Northwest Europe with Diss Mere highlighted by a yellow circle. (b) Photo of the lake and UWITEC coring platform during the coring campaign in 2016. (c) Lake bathymetry with core locations. (d) Catchment map and aerial photograph of the town of Diss and surrounding region, showing elevation (metres above sea level). [Color figure can be viewed at wileyonlinelibrary.com]

Pursehouse, 1961; Peglar, 1993; Yang, 2010). The trade industry and market has remained through time, and the town itself has expanded and today supports a population of just under 10 000 habitants (Fig. 1c). The combination of a rich cultural history around the lake, as well as the well-studied lake sediments with a well-refined chronology (see subsection below), makes it an ideal location to investigate human–environmental interactions through time.

Previous work on Diss Mere sediments

Stratigraphy

The first sediment sequence from Diss Mere was studied in the 1980s with a particular focus on landscape evolution and land use history, described briefly above (Peglar, 1993; Peglar et al., 1984, 1989). In 2016, a new sediment profile for the lake (DISS16) was collected and described in Martin-Puertas et al. (2021). This sediment profile identified three distinct units (Fig. 2a; Supporting Information Fig. S1). Unit 3 (1443–1386 cm) comprises the lowermost sediments containing a matrix of calcareous silts and sands with the presence of pebble-sized clasts (Fig. 2a, c). Unit 2 (1386–957 cm) represents the deposition of biogenic-calcite varves (Zolitschka et al., 2015), and several centimetre-thick turbidite deposits intercalated within the varves. The boundary between Unit 3 and 2 is sharp with a clear transition between the massive sediments and the varve structure. Unit 1 (957–0 cm), the uppermost unit, contains organic-rich mud with periodic micritic carbonate horizons. The preservation of these calcite horizons varies throughout Unit 1 with laminated and faintly laminated sediments intercalated with sections of massive sediments. The transition between Unit 2 and 1 is diffuse with the varved laminations gradually fading out over the last few varves. The Holocene sequence is continuous, with no hiatus identified (Martin-Puertas et al., 2021). The basal sediments of the DISS16 core (represented by Unit 3) are formed of reworked chalky till material and were impenetrable with the coring system, and thus the origin of the lake remains uncertain (Martin-Puertas et al., 2021).

Varve deposition and lake monitoring

Most of the research conducted to date on the DISS16 sediments has focused on the varved sediments (Unit 2) (Martin-Puertas et al., 2021, 2023; Walsh et al., 2021; Harding et al., 2022; Walsh et al., 2023). A typical varve in the record is composed of a light endogenic calcite layer, and a darker organic layer formed of chrysophyceae cysts, organic matter, planktonic centric diatoms and occasional micrite (Peglar et al., 1984). Whilst the varves are consistently classified as biogenic-calcite, variability in the couplet described above are observed – such as extremely thin or missing calcite layers or additional monospecific diatom blooms – and described in detail in Martin-Puertas et al. (2021). The average sedimentation rate (i.e. varve thickness) within this period is 0.04 cm a^{-1}.

A 3.5-year monthly lake monitoring study on the current lake system was applied at Diss Mere to identify the seasonality of the sediment deposition at present (Boyall et al., 2023). This investigation revealed a similar seasonality in the modern depositional processes to those interpreted from the varved sediments (Martin-Puertas et al., 2021, 2023). A clear seasonal cycle of authigenic calcite deposited during the summer when the lake is stratified was identified, followed by the main diatom/organic-rich accumulation of sediments deposited during the autumn and winter whilst the lake is mixing and able to supply nutrients to the epilimnion. Despite the seasonal-driven sediment deposition occurring in the present lake system at Diss Mere, varves are unable to be preserved due to the lack of prolonged anoxia at the base of the lake (Boyall et al., 2023). This means that bioturbation and post-depositional mixing can occur, disturbing the preservation of the seasonal laminations (Zolitschka et al., 2015; Roeser et al., 2021; Boyall et al., 2023).

The Diss Mere varve chronology

The varve chronology for Diss Mere (DISSV-2020) integrates varve counting, radiocarbon dates and a number of tephra layers into a Bayesian depositional model (Martin-Puertas et al., 2021; Walsh et al., 2021, 2023). The varved sequence was deposited between 10 290 ± 55 and 2069 ± 39 cal a BP (Martin-Puertas et al., 2021). The end of varve preservation is well dated by the deposition of the Glen Garry tephra layer (2073 ± 39 cal a BP) deposited at the top of Unit 2 (Martin-Puertas et al., 2021; Walsh et al., 2021). Unit 2 covers most of the Holocene period but, in length, it represents less than one-third of the entire sediment record recovered from Diss Mere.

Materials and methods

The Diss Mere sediment record

Four parallel sediment cores (DISS16-A, B, C and D) were retrieved in September 2016 using a UWITEC piston core system and two UWITEC gravity cores (DISS16-1S and DISS16-2S) to retrieve a continuous profile of the Holocene (Martin-Puertas et al., 2021). All cores were retrieved from the deepest part of the lake with a maximum distance of 5 m (Fig. 1). A 14.50-m-long composite profile was created by matching the different core sections using marker horizons and the best-preserved sections from the overlapping cores (Fig. S1) (Martin-Puertas et al., 2021). The composite depths used within this study include an additional 68 cm to the depths published in Martin-Puertas et al. (2021), Walsh et al. (2021) and Walsh et al. (2023) to account for the additional sediments collected in the gravity core.

Dating

The first 9 m of sediments (Unit 1) were dated by radiometric techniques as annual layer counts were not possible. Surface sediments were analysed for ^{210}Pb, ^{226}Ra, ^{137}Cs and ^{241}Am by direct gamma assay (Appleby et al., 1986) at the Environmental Radiometric Facility at University College London, using an ORTEC HPGe GWL series well-type coaxial low-background intrinsic germanium detector. The calcareous nature of the Diss Mere sediments makes radiocarbon dating challenging because only terrestrial macrofossils provide reliable dates. In the first 9 m of the sequence, three terrestrial macrofossils were found and analysed by accelerator mass spectrometry (AMS) for ^{14}C dating at the Scottish Universities Environmental Research Centre (SUERC, see Table 1 for the terrestrial material used for dating). For the last two millennia, a Bayesian age model was constructed in OxCal (Bronk Ramsey, 2009) using a *P_sequence* depositional model. The model contained Bayesian outlier detection, sediment interpolation and automated calculation of the rigidity of the model (k factor). Model priors included the available radiocarbon dates and their associated depths in the sediment, the IntCal20 curve (Reimer et al., 2020), as well as the ^{137}Cs peak and depth, and core top age (2016 CE). The depth-based model was anchored to the published varve model (DISSV-2020) using

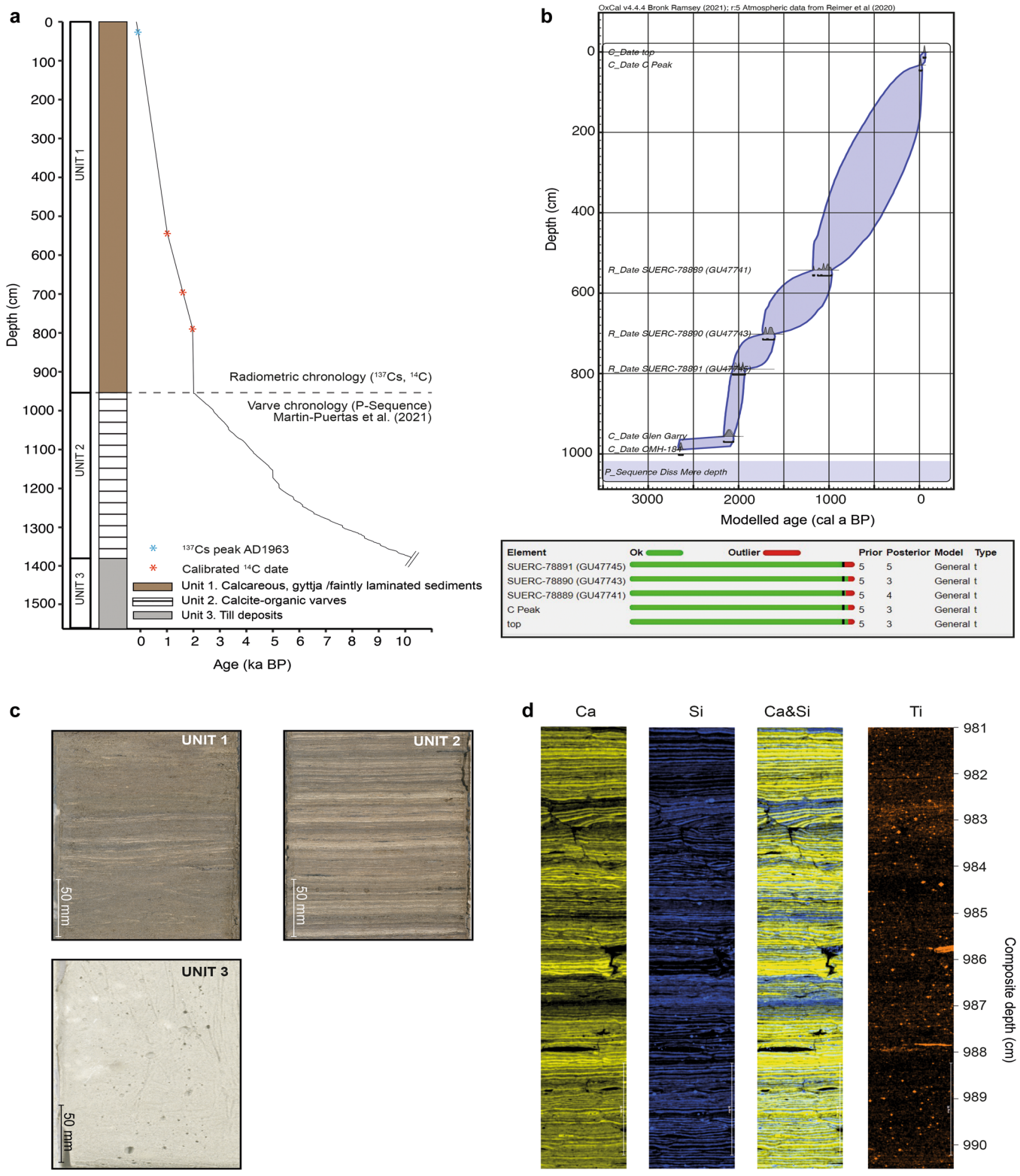

Figure 2. Diss Mere chronology and sediment sections. (a) Sediment units and lithology with the Diss Mere age model, combining the radiometric dates from this study and varve chronology from Martin-Puertas et al. (2021). (b) Age–depth model for the last 2000 years and outlier table. (c) Core photos of the sediments showing deposits in Unit 1 (photo taken at 420–440 cm), Unit 2 (980–1000 cm) and Unit 3 (1490–1510 cm. (d) Tornado element mapping for calcium (Ca), silica (Si), Ca and Si (Ca&Si), and titanium (Ti) on a resin-impregnated sediment block for the sediment depths between 981 and 991 cm. Yellow, blue and orange represent the presence of Ca, Si and Ti, respectively, in the varves. [Color figure can be viewed at wileyonlinelibrary.com]

the modelled ages of the Glen Garry and OMH-185 tephras at their recorded depths (Martin-Puertas et al., 2021).

XRF element scanning

Detailed micro-facies analyses and core descriptions were compared with the chemical sediment composition obtained from both sediment impregnated in epoxy resin used to make thin sections, and the split-core sediment surface. Five epoxy-impregnated sediment blocks were analysed using a M4 Tornado (Bruker), equipped with a Rh X-ray tube operated at 50 kV, 0.6 mA and a dwell time of 50 ms to generate detailed element distribution maps with a resolution of 50 µm to assess the geochemical composition of the seasonal layers.

Table 1. Diss Mere radiocarbon dates used in this study. The calibrated dates were calculated according to the IntCal20 curve (Reimer et al., 2020).

Sample ID	Material	Composite depth (cm)	δ^{13}C relative to VPDB (‰)	Radiocarbon age, BP	Calibrated age, BP (IntCal20)	Error (±)
SUERC-78889	Leaf	542.7	−27	1148 ± 21	1075.5	102.5
SUERC-78890	Leaf	701.8	−26.7	1780 ± 24	1668.5	62.5
SUERC-78891	Wood	789.2	−27.6	2062 ± 21	1996	68

The DISS16 composite profile was scanned using an ITRAX XRF-core scanner (Cox Analytical Systems) at GFZ-Potsdam between 0.7 and 13.8 m depth, corresponding to Units 1 and 2 (Martin-Puertas et al., 2021). Unit 3 was not scanned as it does not contain lake sediments (see 'Stratigraphy' above). Measurements were carried out every 200 µm by irradiating the split-sediment core surface for 10 s with a Cr X-ray source operated at 30 kV and 30 mA. In addition to the continuous scanning, duplicate measurements were taken from at least two selected positions of 1–2 cm length in each core section, providing a total of 1736 positions with three measurements. The elements silica (Si), sulphur (S), potassium (K), calcite (Ca), titanium (Ti), manganese (Mn), iron (Fe) and strontium (Sr) were selected based on the relative standard error (<15%) calculated from the replicate measurements.

Element intensity records commonly acquired by XRF core scanning reflect changes in the sediment composition although they can also be affected by physical sediment properties, sample geometry and measurement time (Tjallingii et al., 2007; Dunlea et al., 2020). Additionally, element intensities are not linearly related to element concentrations due to matrix effects that cause absorption and enhancement effects of the surrounding sediment (Weltje and Tjallingii, 2008; Weltje et al., 2015). However, centred log-ratio (clr) transformation (Aitchison, 1986) accounts for most of these effects (Weltje and Tjallingii, 2008), as well as circumventing complications of statistical analyses when using compositional data (Bertrand et al., 2023) and this approach has been applied to the geochemical record of Diss Mere.

All statistical analyses of the XRF core scanning data were performed after log-ratio transformation using the XELERATE software (Weltje et al., 2015). Statistical groups with similar compositions were characterized by Ward's hierarchical clustering, where each data point is assigned to one of the evenly distributed centre points based on its Euclidian distance and without stratigraphical constraints. For Ward's clustering, the relative difference of each cluster is presented in a dendrogram which discloses potential solutions of including fewer clusters. Using the same software, we also visualize the clustering results overlaid on a principal component analysis (PCA) as well as stratigraphically down core. For the statistical analysis of the XRF data (including the PCAs and hierarchical clustering) we used the original sample resolution to analyse the results. We then subsequently resampled to 1 year for the plotting of element ratios to reduce intra-annual variability and better observe the general geochemical trends through time.

We investigate the sensitivity of the Diss Mere sediment record to temperature variability through comparisons with different Holocene temperature reconstructions, namely the TANN north-west Europe annual temperature reconstruction (Davis et al., 2003), the North Greenland Ice Core Project (NGRIP) δ^{18}O isotope record (Rasmussen et al., 2006), the temp12k reconstruction at 30–60°N and 60–90°N (Kaufman et al., 2020) and the Last Millennium Reanalysis (Tardif et al., 2019). We calculate the relationship between the Diss Mere record and temperature reconstructions through Pearson's correlation coefficients (r) and test for statistical significance using p-values (p). To prevent the effect of autocorrelation in timeseries data exacerbating the significance of correlations, we apply the methods of both Bretherton et al. (1999) to adjust the effective sample size, and Benjamini and Hochberg (1995) to control the proportion of falsely rejected hypotheses. For each of the correlations we resample the Diss Mere data to the resolution of the comparison data. The Diss Mere data are resampled to 100 years for the correlation with temp12k (Kaufman et al., 2020), and to 20 years for the NGRIP record (Rasmussen et al., 2006). Both the Diss Mere record and the Last Millennium Reanalysis (Tardif et al., 2019) are resampled to 50 years to account for the chronological uncertainty in the Diss Mere record. Correlations and adjusted significance testing were completed using R v4.3.1 (R Core Team, 2023) utilizing the 'forecast' package v8.21.1 (Hyndman et al., 2023). Correlations were not possible for the TANN temperature reconstruction of Davis et al. (2003) because the raw data were not available. Instead, the data were digitalized using GraphReader.com and are therefore prone to errors.

Results

Chronology for the last 2000 years in the Diss Mere record

A Bayesian age-depth model (DISS2k) has been created for the first 9 m of sediments representing the last ca. 2000 years (Fig. 2). The Bayesian age–depth model combines radiometric dates (Table 1) with two previously published tephra horizons: the Glen Garry and the OMH-185 (Martin-Puertas et al., 2021; see 'Dating' above) (Fig. 2b).

Equilibrium of total ^{210}Pb activity with supported ^{210}Pb activity is reached at 40 cm of the core (Fig. S2). Unsupported ^{210}Pb activities are relatively low in the sediments (which is possibly due to high sedimentation rates), and they decline irregularly with depth, suggesting changes in the sedimentation rates (see Fig. 2b and Fig. S2). The main peak of ^{137}Cs occurs at 34 cm, which assigns this depth to 1963 CE coinciding with maximum atmospheric fallout from nuclear weapon testing (Fig. S2). The non-monotonic features in the unsupported ^{210}Pb profile precluded the use of the constant initial concentration (CIC) dating model, and the final CRS model accepts the ^{137}Cs peak only.

The sedimentation rate during the varve preservation is 0.04 cm a^{-1} (Martin-Puertas et al., 2021). However, the results of the DISS2k age–depth model reveals a rapid increase in sedimentation rate between the deposition of the Glen Garry tephra located at the top of the varved sequence (956.5 cm) and the oldest ^{14}C date (789.2 cm) to 1.45 cm a^{-1}. There are no reported outlying dates in the Bayesian outlier detection which supports a very rapid and large shift in sedimentation rate when the varves stop preserving. Above the lowermost radiocarbon date, the sedimentation rate declines to 0.27 cm a^{-1} within the first millennium of the common era and slightly increases again to 0.46 cm a^{-1} during the last millennium (Fig. 2b).

XRF scanning and multivariate analysis

By combining the element-mapped composition of the seasonal laminations (Fig. 2d) and the composition and timing of modern sediment deposition (Boyall et al., 2023), we identify seasonality in the Diss Mere sediments using the elements Ca, Si, Fe and Ti. These elements are used as potential proxies as follows: Ca as a

proxy for authigenic calcite precipitation, which is mostly deposited in the pale summer layer; Si as a proxy for biogenic silica and diatom productivity, which is deposited in the darker organic winter layer; Fe as a proxy for redox conditions; and Ti as a proxy for detrital input.

Element concentrations were explored using a biplot of principal components (PC) 1 and 2 explaining 69.7% and 14.7% of the total variance, respectively (Fig. 3). With respect to PC1, elements associated with authigenic carbonate (Ca and Sr) have positive values, and those with detrital sediment (Ti, K and partly Fe) have negative values. This suggests that PC1 reveals relative variations between authigenic carbonates and detrital in-wash, which can be indicated by ln(Ca/Ti). Although less pronounced than Ca, positive PC1 values are found for the element Si representing biogenic silica deposition in autumn and winter months. The opposite orientation of Si to the detrital elements reveal that these elements are negatively correlated, further supported by the correlation matrix in Table 2a. This would suggest that the ln(Si/Ti) record could be used to explain relative changes between diatom productivity and detrital lake sediments. However, when the correlation matrices are divided stratigraphically, the correlations between these elements become more variable (Table 2b–d). The positive correlations between Si and Ti for parts of the record (between 525 and 68 cm) indicate that Si is entering the lake through detrital sources and thus the ln(Si/Ti) record cannot be used throughout the full record to explain diatom productivity.

The variation on PC2 shows strong positive loadings for the redox-sensitive element, Fe, and negative values for the detrital elements K and Ti. This may suggest that PC2 reveals the relative variation between detrital and reduced sediments, which can also be indicated by ln(Fe/Ti).

The six-cluster solution represents the optimum number of statistical clusters matching both the lithology and chemical variations of the DISS16 record (Fig. 4). The relative differences in the compositional characteristics of the six clusters are visualized on both the dendrogram (Fig. 3a) and the PCA biplot (Fig. 3b). The cluster results show a similar distribution along PC1 (Fig. 3b) with strongly positive values for cluster 6 (red) shifting to slightly positive values for cluster 4 (green), to slightly negative values for cluster 3 (light blue), to strongly negative values for cluster 1 (dark blue). The clusters show a clear distribution from detrital-dominated sediments (cluster 1) to carbonate-dominated sediments (cluster 6).

Based on the stratigraphic position of the clusters we have assigned three distinct geochemical units (GUs) to the sediment profile (Fig. 4): GU1, 2 and 3 from the basal sediments to the surface. GU1 (1378–957 cm) coincides with sedimentological Unit 2 in the DISS16 sequence (i.e. varved sediments, see 'Straigraphy' above). Cluster 6 classifies these sediments alternating with cluster 5 (Fig. 4). At the base of GU1, cluster 3 appears frequently with the occasional appearance of cluster 2. We mark the presence of these clusters as a sub-unit GU1a (Fig. 4). GU2 (957–525 cm) coincides with the lower part of sedimentological Unit 1 after the varved sediments and is associated with cluster 4. The sediment within GU2 is composed of olive-green mud with occasional faint calcite laminations (Fig. S1; Martin-Puertas et al., 2021). The transition between GU1 and GU2 is marked by an increase in background Ti input into the lake (Fig. 4). GU3 (525–68 cm) corresponds to the uppermost 5 m of sediments and the upperpart of sedimentological Unit 1. However, unlike GU2, the dominant geochemical cluster within GU3 is cluster 1, which is associated with clastic elements. Cluster 3 returns periodically at the top of this zone, forming an additional subunit (GU3b). Similarly to the previous transition, the change from GU2 to GU3 is also marked by an increase in Ti (Fig. 4). The cluster-based geochemical units therefore reflect a shifting lake system from carbonate to clastic sediment deposition. Adopting this approach has revealed greater variability within the sediments that was not apparent from the core descriptions alone (Fig. S1), emphasizing the advantage of combining multiple proxies to investigate depositional change.

Discussion

Holocene lake evolution

The Diss region has been occupied continuously for several thousand years (Peglar, 1993), and the interactions between human activity and Holocene climate evolution adds complexity to interpreting drivers of change recorded in the Diss Mere

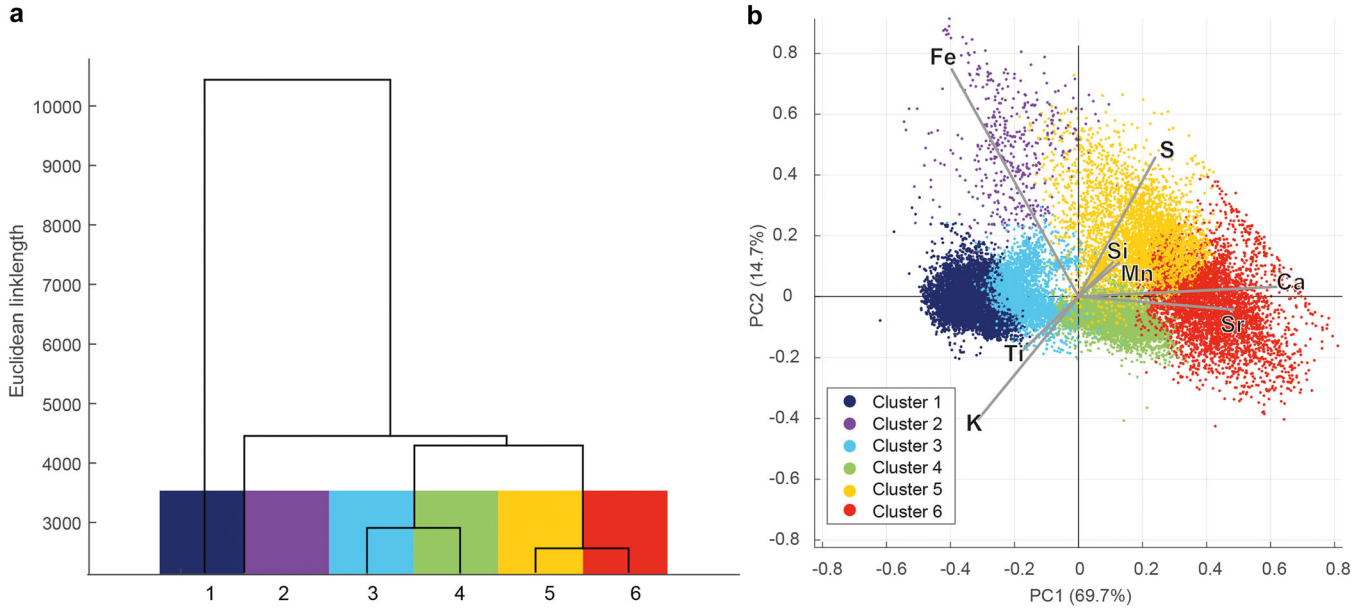

Figure 3. Statistical analyses of the DISS16 XRF core scanning measurements. (a) Dendrogram of the six-cluster solution using Ward's hierarchical clustering. (b) PCA biplot of PC1 and PC2 for selected XRF elements (S, Si, K, Ca, Ti, Mn, Fe, Sr) including the relative element correlations as well as the distribution of the data points and statistical clusters. [Color figure can be viewed at wileyonlinelibrary.com]

Table 2. Correlation matrices for selected XRF core scanning elements for the full stratigraphic record and for each geochemical units (GU). (a) Correlation matrix for the full stratigraphic record used in this study, (b) correlation matrix for GU1, (c) correlation matrix for GU2 and (d) correlation matrix for GU3. The correlation analysis used the clr-transformed elements, and all correlations were calculated on depth at a 1-cm resolution. *n* indicates the number of depths used in the correlation matrix.

(a) Full stratigraphic record (1378–68 cm) $n = 1312$

	Si	Ca	Ti	Mn	Fe	S
Si	1					
Ca	0.54	1				
Ti	−0.59	−0.78	1			
Mn	0.39	0.49	−0.53	1		
Fe	0.01	−0.36	0.25	−0.08	1	
S	0.52	0.72	−0.70	−0.52	0.001	1
K	−0.31	−0.53	0.68	−0.56	0.37	−0.58

(b) GU1 (1378–957 cm) $n = 426$

	Si	Ca	Ti	Mn	Fe	S
Si	1					
Ca	0.24	1				
Ti	−0.43	−0.56	1			
Mn	0.25	0.18	−0.40	1		
Fe	0.14	−0.35	0.10	0.14	1	
S	0.15	0.22	−0.24	0.40	0.67	1
K	−0.04	0.21	0.30	−0.43	−0.13	−0.08

(c) GU2 (957–525 cm) $n = 431$

	Si	Ca	Ti	Mn	Fe	S
Si	1					
Ca	0.51	1				
Ti	−0.16	−0.35	1			
Mn	0.30	0.21	−0.10	1		
Fe	0.21	−0.15	0.66	0.11	1	
S	0.26	0.58	0.21	0.19	0.42	1
K	0.09	0.04	0.78	−0.05	0.69	0.48

(d) GU3 (525–68 cm) $n = 455$

	Si	Ca	Ti	Mn	Fe	K
Si	1					
Ca	−0.02	1				
Ti	0.66	−0.45	1			
Mn	−0.10	0.42	−0.34	1		
Fe	0.20	0.38	−0.08	0.48	1	
S	0.13	−0.04	0.06	0.12	−0.07	1
K	0.70	−0.02	0.84	−0.30	−0.01	−0.04

sediments. By combining palaeolimnological analyses with published information about human occupation in the region, we have identified three distinct phases in the lake's history (Fig. 5e): (i) a phase with low human influence on the lake (GU1; 10 290–2070 cal a BP), (ii) a phase with intermediate human activity (GU2; 2070–1040 cal a BP) and (iii) a phase with intensified human activity (GU3; 1040 cal a BP – present). We discuss these three phases in the following sections.

Low human influence (10 290–2070 cal a BP)

According to the pollen record from Diss Mere, only isolated changes occurred in the lake catchment prior to ca. 2000 cal a BP (Peglar, 1993; Fig. 5c, d). This phase with the lowest human influence (GU 1 and Unit 2) marks the period where lake sediments started accumulating as biogenic-calcite varves. The high temporal (seasonal) resolution of the sediments, combined with the element mapping shown in Fig. 2(d), reveals that Ca and Si are sorted by the seasonal layers. The summer calcite layer is geochemically represented by Ca, whilst the darker winter organic layer is mostly represented by Si and is associated with the diatom blooms. The high-amplitude variability of the ln(Ca/Ti) and ln(Si/Ti) during this stage of the lake therefore represents interannual variability (Fig. 5). Ti_{clr} is used to represent annual detrital input to the lake. During this phase, Ti_{clr} values are relatively low in comparison to the last two millennia (Fig. 5).

Biogenic-calcite varves are preserved through Unit 2. However, clusters 2 and 3, which predominantly represent clastic sediments (i.e. negatively correlated with PC1, Fig. 3), occur at the base of this unit within GU1a between 10 290 and ca. 8100 cal a BP (1386–1300 cm). This suggests that although varves are still forming and preserving, the sediments might have a different source. Ti_{clr} values are higher during GU1a (supporting the interpretation that these clusters contain a clastic component), and consequently the element ratios ln(Ca/Ti) and ln(Si/Ti) decrease (Fig. 5). Low seasonal calcite precipitation in the first 2000 years of the lake's history is supported by microfacies analysis showing a much thinner varve thickness than the long-term average (0.01 cm a^{-1} compared to the mean of 0.04 cm a^{-1}) because of a very thin or absent calcite layer (Martin-Puertas et al., 2023). This suggests that the carbonate accumulated in the sediments during GU1a (as represented by Ca_{clr}) might have a detrital origin – either through runoff or wind erosion – because Diss Mere is a marl lake. The interpretation of increased detrital material is supported by the pollen record, which revealed the presence of several shade-intolerant herbs and non-arboreal pollen at this time (Peglar et al., 1989), suggesting that there were areas without woodland cover in the Early Holocene (Fig. 5c, e). After this interval, the sediments between ca. 8100 and 2070 cal a BP are mostly characterized by cluster 6 (authigenic carbonate driven) representing the well-preserved varves. As a precondition for varve formation and preservation, lakes must have sustained periods with an anoxic hypolimnion to limit bioturbation and post-depositional mixing (Roeser et al., 2021; Zolitschka et al., 2015). An anoxic hypolimnion results from either an optimum lake surface–depth ratio which is able to sustain thermal and chemical stratification, or eutrophic waters with both high productivity and organic matter decomposition (Żarczyński et al., 2019; Zolitschka et al., 2015). Increased lake productivity caused by human activity and nutrient loading has resulted in a shift to more hypoxic–anoxic conditions in lakes globally (Jenny et al., 2016). For the Holocene varves in Diss Mere between 10 290 and 2070 cal a BP, limnological evidence suggests that anoxic hypolimnetic conditions were maintained by an optimum lake morphometry, where the depth of the lake was sufficient to enable thermal and chemical stratification and limit full mixing of the water column, rather than eutrophic conditions. The evidence for this interpretation can first be seen in the sediment record where the transition from varves to non-varved sediments is diffuse with laminations fading out over the last four varves (Martin-Puertas et al., 2021), suggesting that the lake gradually infilled and shallowed (Boehrer and Schultze, 2008). The infilling would have allowed prolonged periods of complete turnover and enabled longer periods of oxygen saturation in the lake, similar to the lake mixing regime seen in the lake today (Boyall et al., 2023). In addition, the lake monitoring survey showed that seasonally laminated deposits respond directly to the limnological seasons (stratification and turnover), and climate parameters such as temperature and

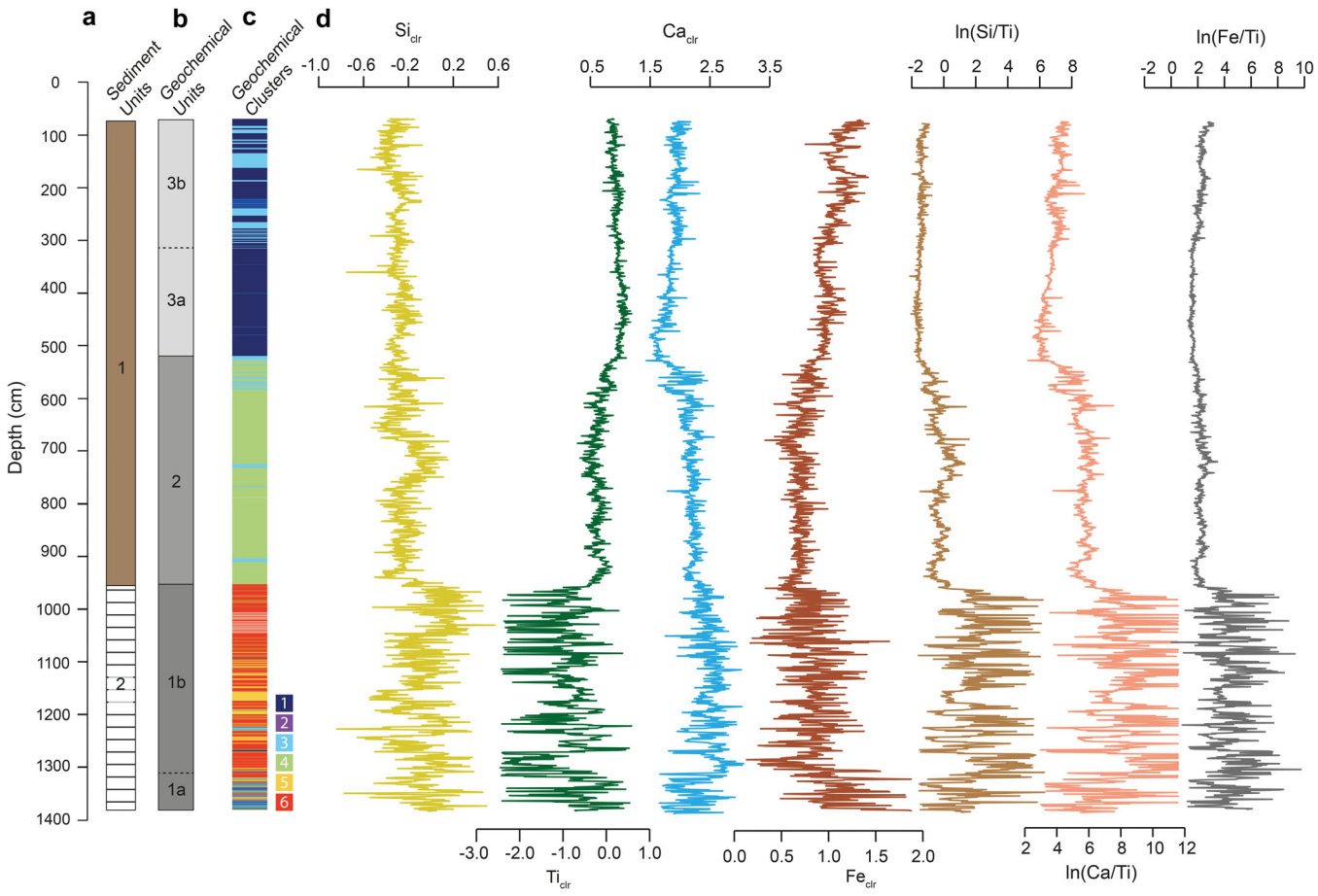

Figure 4. Diss Mere stratigraphic geochemical information used in this study, including (a) lithology of the main sedimentary units, (b) geochemical units, (c) stratigraphic position of different geochemical clusters, and (d) stratigraphic geochemical records for the element ratios Si_{clr}, Ti_{clr}, Ca_{clr}, Fe_{clr}, ln(Si/Ti), ln (Ca/Ti) and ln(Fe/Ti). [Color figure can be viewed at wileyonlinelibrary.com]

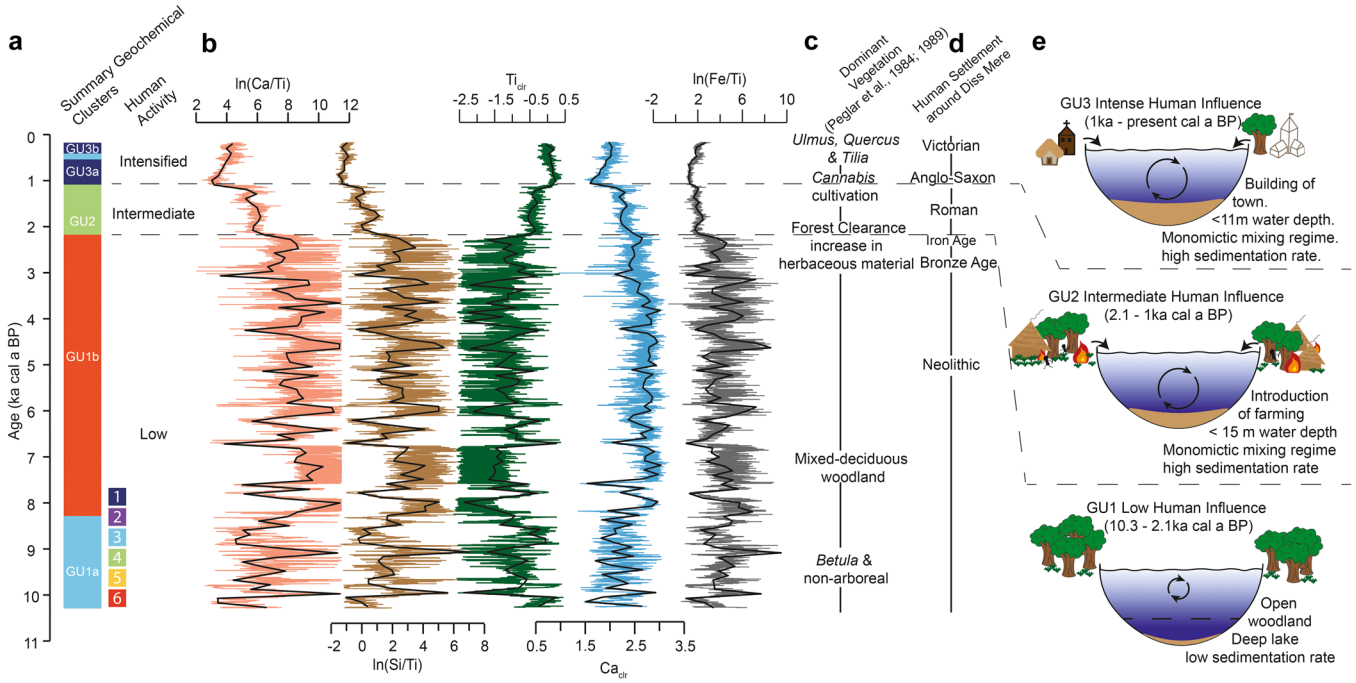

Figure 5. Summary of geochemical information and human activity at Diss Mere. (a) Summary of the clustering results based on the characteristic cluster associated with each time period and classifications of levels of human activity. (b) Element ratios and central-logged elements plotted against age at 1-year resolution for ln(Ca/Ti), ln(Si/Ti), Ti_{clr},Ca_{clr} and ln(Fe/Ti), resampled to 100 years overlaid in black. (c) Timeline of palynological findings from Peglar et al. (1984, 1989). (d) Historical timeline of human presence around Diss Mere. (e) Lake model for the different stages of human activity. [Color figure can be viewed at wileyonlinelibrary.com]

wind eventually (Boyall et al., 2023). This suggests that the depositional processes during most of the Holocene and present are similar, but the preservation controls are not favourable in the lake today, despite the lake being highly productive.

Elemental compositions and element ratios have been used to trace changing oxygen availability in lakes, such as ln(Fe/Mn) (e.g. Engstrom et al., 2006; Martin-Puertas et al., 2017, Żarczyński et al., 2019), ln(Mn/Fe) (e.g. Naeher et al., 2013; Evans et al., 2019; Makri et al., 2021), ln(Fe/Ti) (e.g. Aufgebauer et al., 2012; Peti and Augustinus, 2022) and sulphur (S_{clr}) (e.g. Żarczyński et al., 2019). However, caution is required when using different geochemical proxies because factors such as detrital in-wash, groundwater inflow and biological activity can influence the oxygen signal within a lake (Jouve et al., 2013; Żarczyński et al., 2019). According to the biplot shown in Fig. 3(b), variability in the anoxic/oxic conditions at the lake bottom were captured best by the ln(Fe/Ti) record from Diss Mere. Under reducing conditions, the available Fe is more soluble as it is reduced to its ferrous state (Fe^{2+}), limiting its ability to precipitate (Davison, 1993), and therefore it can be used to trace oxygen availability. However, Ti is redox-insensitive, and therefore, by normalizing against Ti, it should allow only the redox element – in this case Fe – to be traced (Żarczyński et al., 2019). This means that periods of higher ln(Fe/Ti) indicate reducing conditions with anoxic bottom waters, and periods of low ln(Fe/Ti) represent oxic conditions. Whilst variable in the Diss Mere sediments, the oxygen availability shows a decreasing trend through the Holocene, reflecting the gradual shallowing of the lake. This shallowing makes the lake more susceptible to oxygen presence in the hypolimnion and thus results in the subsequent cessation of varve preservation at the end of this phase (Fig. 5b, e).

It is of note that cluster 5 appears occasionally through GU1b, especially during the Mid-Holocene. This cluster is associated with in-wash deposits intercalated within the varved sequence (Martin-Puertas et al., 2021; Fig. S1) and is characterized by low ln(Fe/Ti) and high Ti_{clr}, supporting the interpretation of sediment deposition from the catchment and littoral parts of the lake (Figs. 4 and 5).

Intermediate human influence (2070–1040 cal a BP/120 BCE to 910 CE)

The second phase of Diss Mere lake evolution is associated with intermediate human activity from the Late Iron Age through the Roman period and into the Late Anglo Saxon period in Britain (Needham, 2007; Hingham and Ryan, 2010). The geochemical composition of the sediments for this phase is more stable than the preceding phase (Fig. 5). Fewer alternations between clusters are observed, and there is less interannual variability of element ratios, probably because the varves were not preserved. The major change that leads to the transition to a new lake environment in this phase is an increase in detrital material from the catchment. This transition is shown by increases in both the Ti_{clr} record and an increase in the sedimentation rate from 0.04 cm a^{-1} in the varved sediments to 1.45 cm a^{-1} for the first few hundred years, and then a reduction to 0.26 cm a^{-1} for the rest of this phase (Fig. 2b). The timing of this change occurred within the latter part of the Iron Age in Britain (Yeloff et al., 2007; Waller and Schofield, 2007). Palynological investigations from previous studies of Diss Mere (Peglar, 1993) complement this interpretation of landscape change by revealing a reduction in woodland and scrub, and a shift towards herbaceous grassland with the occurrence of cereals (Fig. 5c, e). The occurrence of cereals at the same time as the shift in lake sediments suggests that these changes were probably driven by human activity. Both the clearance of woodland surrounding the lake and wider land-use changes in the catchment would have caused the soils to be less stable and increase erosion of sediment into the lake, resulting in rapid infilling. Alternatively, or in combination, the loss of forest cover could have exposed the lake to winds and enhanced the ability for wind-driven turbulence. This exposure encourages lake mixing through the creation of surface waves and subsequent turbulence allowing more of the lake's surface to absorb oxygen from the atmosphere (Bouffard et al., 2014). As a result, during periods when the lake is not thermally stratified and lake turnover occurs, oxygen is translocated down the water column and able to reach the bottom of the lake (Makri et al., 2020; Żarczyński et al., 2019).

The geochemical, sedimentological and palynological changes observed within this phase mark the first noticeable evidence of human activity on lake functioning at Diss Mere. Similar changes at ca. 2000 cal a BP have been observed in other lake records from around Europe, including both the cessation (e.g. Meerfelder Maar, Martin-Puertas et al., 2012) and formation (e.g. Lake Montcortès, Corella et al., 2011; Rull et al., 2021) of varved sediments, significant changes in vegetation assemblages (e.g. Lake Wonieść, Dörfler et al., 2022 and Lake Moossee, Makri et al., 2020), as well as distinct changes in lake sediment geochemistry (e.g Kamyshovoe Lake, Druzhinina et al., 2022).

Intensified human influence (1040 cal a BP/910 CE to present)

The third and final phase of lake evolution in the Diss Mere record is characterized by intensified human activity. This phase begins at the transition between GU2 and the beginning of GU3, marked by a further increase in Ti_{clr} (Fig. 5) and a dominance of mostly cluster 1 (associated with detrital sediments, Figs. 3 and 4). This phase coincides with the Late Anglo Saxon period and the onset of the Medieval period, at which the building of the historic market town of Diss began (Fig. 5e, Fritz, 1989; Higham and Ryan, 2010). Vegetation shifts were apparent at the beginning of the phase representing large open arable fields, which have been related to increased population and resource demands (Peglar, 1993). The marked increase in detrital material occurred at the beginning of this phase, coinciding with the periodic occurrence of cluster 3 (Fig. 5). The ln(Fe/Ti) record remains the same as during GU2, probably because oxic conditions at the lake bottom prevailed through most of the year as the lake was that not deep enough to maintain permanent anoxia (Boyall et al., 2023).

Productivity and calcite precipitation over the last two millennia

During the last two millennia (GU2 and GU3), human-induced detrital input and sediment infilling caused changes in the lake oxic regime and varve preservation, and led to lake eutrophication (Fritz, 1989). This change is marked by a shift in the diatom communities, mostly seen in the transition from *Cyclotella*-dominated species to *Stephanodiscus* sp. after the cessation of varves in response to increased dissolved and particulate external nutrient input (Fritz, 1989). Despite the interpretation of a switch to eutrophic lake waters recorded by the diatom record, neither Si_{clr} nor ln(Si/Ti) shows an expected increase in diatom productivity (Figs. 4 and 5). For this part of the Diss Mere record, the relationship between detrital and siliclastic material is positive (Table 2). This suggests that some of the silica originates from the catchment and could explain why the ln(Si/Ti) record does not reflect the change in diatom

communities and productivity in the lake. In addition, the increases in domestic waste due to larger, more complex and permanent human settlements from the Late Iron Age to the present could have reduced the concentration of Si relative to nitrogen or phosphorous (Ryther and Officer, 1981), which would explain the change from *Cyclotella* sp. to *Stephanodiscus* sp. 2000 years ago. The proportion in which nutrients are loaded to a system can exert a strong influence on what algal species will thrive (Hecky and Kilham, 1988), for example the occurrence of blue-green algae inhibiting the growth of diatoms (Keating, 1978). Diss Mere currently has a high concentration of blue-green algae, signalling lake eutrophication. This eutrophication could explain the gradual decrease in diatom productivity reflected in the geochemical proxies in GU2 and GU3 over the last two millennia of the lake's history (Fig. 5).

Despite the shifts observed in the productivity of Diss Mere, and the gradual shallowing of the lake basin, authigenic calcite precipitation (ln(Ca/Ti) and Ca_{clr}) gradually decreased over the last two millennia (Fig. 5). This trend is opposite to what may be expected with eutrophication as eutrophication results in a higher lake water pH which is a driver of calcite precipitation (Kelts and Hsu, 1978). Additionally, a reduction of the water volume as a result of gradual sediment infilling would also favour increased calcite precipitation by saturating the water with a greater amount of available Ca (Pleskot et al., 2018). Because the opposite has happened at Diss Mere, and authigenic calcite gradually decreased (Fig. 4), it suggests that neither productivity and/nor shallower water is a driver of calcite precipitation. This suggests that calcite precipitation might still be driven by temperature changes during the stratification season – a proposal that is supported by the monitoring survey which found the greatest amount of calcite precipitation when temperatures are higher (June to August), rather than when lake productivity is strongest (September, October and February) (Boyall et al., 2023). We further explore the sensitivity of the geochemical record to temperature at Diss Mere below.

Exploring the sensitivity of the geochemical record to temperature

Previous investigations using the Diss Mere varves reveal a clear proxy response of the lake to climate variability. For example, a high-resolution diatom record from Diss Mere showed that the diatom assemblages responded to regional wind direction and strength during a Late Holocene climate oscillation 2800 years ago (Harding et al., 2022). In addition, the varve thickness record showed a good correlation to the simulated Atlantic Meridional Overturning Circulation (AMOC) and annual averaged surface temperature, resembling decadal- to millennial-scale climate variability in the North Atlantic region (Martin-Puertas et al., 2023). These climate links to the Diss Mere sediments provide scope to investigate any potential climate signals recorded in the geochemical record presented in this paper. We propose that the Ca_{clr} record is the most likely geochemical proxy for temperature as: (i) the main deposition of Ca occurs within the seasonal calcite layer precipitated during the summer (Fig. 2d), and (ii) the thickness of the calcite layer preserved in the varved sediments correlates to mean annual temperature ($r = 0.52$, Martin-Puertas et al., 2023), although a bias towards the summer season might be present. We sought to test whether the Ca accumulated in the Diss Mere sediments was sensitive to temperature variability and, if so, whether the analysis of the XRF core scanning data offers the opportunity to explore and extend the climate record of Diss Mere until the present, which so far is only based on the period before the last two millennia when varve preservation ceases.

The precipitation of calcite in lakes can be a function of CO_2 uptake from photosynthetic organisms, favourable water temperatures or both (Dittrich and Obst, 2004; Plummer and Busenberg, 1982). The modern lake monitoring of Diss Mere revealed that calcite precipitates throughout the full year due to oversaturation of Ca within the lake water. However, peaks in calcite precipitation (coarser grains) occur during the summer months when temperatures are highest in July–August and a secondary smaller flux of calcite (fine grains) follows with autumnal diatom blooms (Boyall et al., 2023). The calcite layers preserved in the varves also show grading in calcite grain size, with finer grains deposited at the top of the varve (Martin-Puertas et al., 2021; Boyall et al., 2023). This pattern suggests that the variability of calcite layer thickness in Diss Mere includes the summer (primary) and the early autumn (secondary) calcite precipitation events. The calcite layer thickness correlates well with the Holocene temperature evolution (Martin-Puertas et al., 2023).

We calculated correlation coefficients between the Ca_{clr} record and the thickness of the varve calcite layer and compared the output with available proxy-based Holocene temperature reconstructions. We used the TANN northwest European temperature reconstruction (Davis et al., 2003), proxy-based temp12k reconstruction for latitudinal bands 30–60°N ($r = 0.66$, $p = 0.12$) and 60–90°N ($r = 0.34$, $p = 0.16$) (Kaufman et al., 2020), and the temperature-sensitive $\delta^{18}O$ record for the northwest European region from NGRIP ($r = 0.35$, $p < 0.005$) (Rasmussen et al., 2006). Considering that we are comparing a variety of proxy records linked to different chronologies and from a wide latitudinal and longitudinal band, the correlations are clear with all curves following similar trends (Fig. 6). The similar trends observed between Ca_{clr} and calcite layer thickness (Fig. 6c) suggest that both thicker calcite laminations and higher Ca_{clr} could be a response to warmer years, reflecting temperature variability in the eastern part of the UK where Diss Mere is located. Because Diss Mere experienced a higher level of human activity during the last 2000 years and varves stopped preserving, we assess the relationship between the carbonate accumulated in the lake and temperature by correlating the Ca_{clr} record with the Last Millennium Reanalysis (LMR) temperature anomalies (Tardif et al., 2019) for an approximated grid around Diss Mere to test whether the Ca_{clr} record is still sensitive to temperature variability despite the increased human activity (Fig. 6d).

Northwest European temperatures in the earliest stages of the Holocene (10 290–7000 cal a BP) mostly reflect gradual climate amelioration responding to the disintegration of Northern Hemisphere residual ice sheets, and increasing solar insolation (Cartapanis et al., 2022; Osman et al., 2021). Most of the records presented in Fig. 6 are consistent with gradually increasing temperatures for the first several thousand years (Fig. 6). However, the Ca_{clr} record from Diss Mere shows a less gradual change. Additionally, in the first part of the record until 8100 cal a BP calcite has a detrital origin (Fig. 5), which may mean that superimposed onto the climate-sensitive Ca_{clr} record is a signal reflecting catchment variability.

Following 8100 cal a BP, the origin of calcite switches to predominantly authigenic precipitation. Ca_{clr} continues to increase and probably reflects rising temperatures. Maximum Ca_{clr} values are recorded at ca. 7200 cal a BP and remain relatively high until ca. 4000 cal a BP (Fig. 6). The maximum Ca_{clr} values during the Mid-Holocene – indicating higher temperatures – are consistent with discussions around a Holocene Thermal Maximum (HTM). The timing of the suspected HTM has been shown to be spatially complex globally with different records revealing maximum temperatures at different times

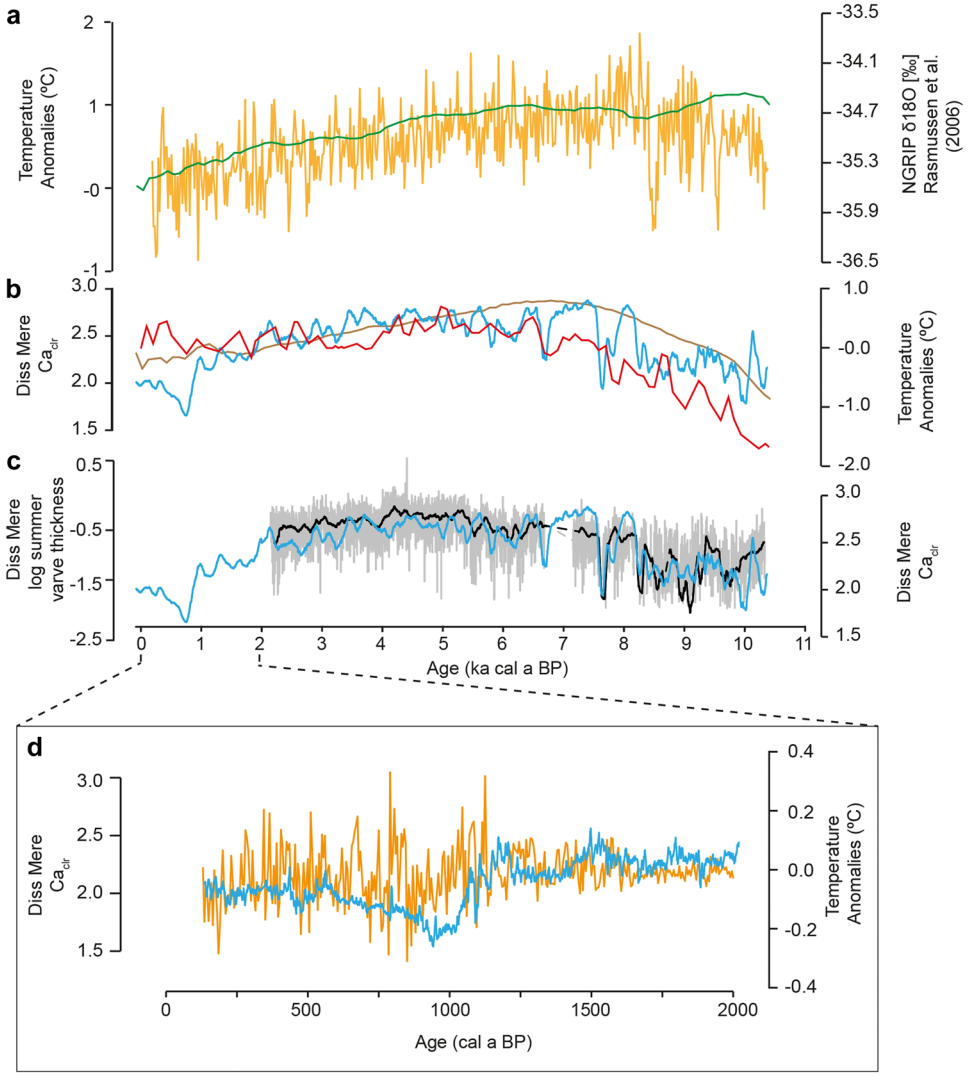

Figure 6. Timeseries of temperature-sensitive records from northwest Europe. (a) High-latitude temperature records with a 100-year moving average NGRIP $\delta^{18}O$ record (yellow) and 500-year moving average temp12k temperature reconstruction for 60–90° N (green). (b) Mid-latitude temperature records with the Ca_{clr} record from Diss Mere as a 100-year resolution moving average (blue), 200-year TANN temperature reconstruction for northwest Europe (red) and 500-year moving average temp12k temperature reconstruction for 30–60° N (brown). The data for the TANN temperature reconstruction was digitalized using GraphReader.com. (c) The Diss Mere log summer varve thickness record (grey) overlaid with a 100-year moving average log summer varve thickness record (black) and 100-year moving average Ca_{clr} record. (d) The last 2000 years with a 5-year moving average Ca_{clr} record from Diss Mere (blue) and the Last Millennium Reanalysis temperature anomalies for 40–60° N and −5° W to 5° E (orange). [Color figure can be viewed at wileyonlinelibrary.com]

(Cartapanis et al., 2022). The 60–90°N temp12k reconstruction records the earliest timing of the HTM at the beginning of the Holocene, followed by the NGRIP $\delta^{18}O$ record which shows the HTM between ca. 9000 and 8000 cal a BP. The early temperature peaks in these high-latitude climate reconstructions have been ascribed to the higher solar insolation received at the poles compared to the mid-latitudes (Kaufman, 2004). The mid-latitude records show maximum temperatures occurring later: temperatures in the 30–60°N temp12k reconstruction peak at ca. 6500 cal a BP and in the TANN reconstruction at ca. 5000 cal a BP. For Diss Mere, the Ca_{clr} record reveals high values spanning a longer period between ca. 8000 until 4500 cal a BP, although with some variability and sharp decreases within this time (Fig. 6). Some discussions surrounding the HTM suggest that an HTM signal is only recorded in proxy records which have a summer bias (Liu et al., 2014; Bova et al., 2021). Given that the Ca_{clr} record from Diss Mere suggests Mid-Holocene warming, it may support the seasonal bias hypothesis and could be explained by the fact that most of the Ca record primarily reflects temperature-induced calcite precipitation in summer (Boyall et al., 2023).

The similarity between the low-frequency Holocene temperature records and the Diss Mere Ca_{clr} record supports interpretations that the lake was sensitive to climate variability through its varved history. However, the results of this study reveal that human activity had a strong influence on lake functioning over the past 2000 years, potentially disrupting the sensitivity of Ca_{clr} as a proxy for temperature. Although the resolution of the LMR is annual, the correlation between Ca_{clr} and the LMR has been calculated at a 50-year resolution to account for some of the chronological uncertainty from the Diss Mere record over the last two millennia. Whilst the weaker chronological precision here may result in lower correlations, the correlation coefficient between the LMR and Ca_{clr} is significant ($r = 0.50$, $p < 0.005$). This highlights that the Ca_{clr} record continues to resemble the reanalysis temperature variability during the last two millennia. However, despite this, there are some differences in the amplitude of variability between both timeseries. For example, both show proportional variability between 2000 and 1000 cal a BP, but in the second millennium of the common era (1000 cal a BP to present) the amplitude of variability in the LMR is increased (Fig. 6).

At approximately 1100 cal a BP, both records reveal a change in their mean values (Fig. 6d). In the Diss Mere record, the difference in the mean values between the first and second millennium of the common era is more substantial than in the LMR and is probably influenced by the impact of intensified human activity on the geochemical composition of the Diss Mere sediments. However, the significant correlation to the LMR remains. This is an interesting and important finding as it highlights that even when Ca_{clr} could be considered a Holocene temperature proxy from the Diss Mere record, the proportionality of the temperature-proxy relationship is not stationary through time. In other words, the amplitude of temperature changes may not be comparable between the three lake phases identified in this study due to the influence of human activity on the lake. Thus, further work would be required to fully assess the relationship between climate and the geochemical record at Diss Mere with the superimposed human influence over the past 2000 years.

Conclusions

This investigation combines XRF core scanning data and sedimentological information from Diss Mere, a lake in Norfolk, UK, to identify the changes in lake evolution, climate trends and human activity through time.

The three phases of lake evolution and human activity, identified through the geochemical and sedimentological records, highlight the complex interactions between climate and human forcing. The minimal disturbance from human activity in the earliest phase allowed the lake to respond naturally to changing seasonal fluctuations in the climate system, and long-term Holocene climate evolution. The second phase with intermediate human activity demonstrated the role that human activity had on the functioning of the lake. The beginning of this intermediate phase was marked by the end of the preservation of varved sediments due to the influx of detrital material through landscape changes relating to increased human activity. The third phase represents the most significant changes to lake functioning coinciding with intense human activity and the building of the town of Diss during the Early Medieval period.

The results from this investigation have shown a clear interplay between humans and the environment leading to a distinct superimposed signal of human activity on the geochemical record. However, by identifying the timings of more intense human activity at Diss Mere, a better interpretation of the sensitivity of the lake to climate can be made. These results provide support for further methodological developments for the analysis of the climate signal from Diss Mere.

Author contributions—L.B. and C.M.P. conceptualized the study. L.B. wrote the manuscript and conducted the formal analysis of the study with assistance from C.M.P. and R.T. R.T. conducted the geochemical analysis and produced the database. S.P.E.B. ran the Bayesian age–depth model. C.M.P. and A.M.M. were involved in the supervision of L.B. All co-authors were involved in the discussion of the data and contributed to the writing and the review of the manuscript.

Acknowledgements. This study was funded by the Royal Society through a Dorothy Hodgkin Fellowship (ref: DH150185) and UKRI contributing to the project DECADAL 'Rethinking Palaeoclimatology for Society' (ref: MR/W009641/1). Laura Boyall is funded by Royal Holloway University of London through a PhD studentship. The authors thank Poppy Harding, Jose Valcárcel and Amy Walsh, who work on the Diss Mere record and have generated data and results used in this study, and Paul Lincoln for previous discussions on data analysis. We thank Bernd Zolitschka, Paul Zander and an anonymous reviewer for their helpful and insightful comments of the manuscript.

Data availability statement

The data that support the findings of this study are available from the corresponding author upon reasonable request.

Supporting information

Additional supporting information can be found in the online version of this article.

Supplementary Figure 1. Diss Mere composite stratigraphic record against depth. With core photos, facies, and geochemical units adapted Martin-Puertas et al. (2021). The uppermost 160 cm are not included due to the moisture content of the sediments causing reflections in the core images.

Supplementary Figure 2. Concentration of radionuclide fallout profiles. a) total ^{210}Pb (blue rhombus) and supported ^{210}Pb (pink line), b) unsupported ^{210}Pb (blue rhombus), and c) ^{137}Cs (rhombus) and ^{241}Am (triangles) concentrations versus composite depth from Diss Mere.

Abbreviations. XRF, X-ray fluorescence; CLR, centred-log ratio; PCA, principal component analysis; NGRIP, North Greenland Ice Core Project; LMR, Last Millennium Reanalysis; CIC, constant initial concentration; PC, principal component; GU, Geochemical Unit; AMOC, Atlantic Meridional Overturning Circulation; HTM, Holocene Thermal Maximum.

References

Aitchison, J. (1986) *The Statistical Analysis of Compositional Data*. Chapman & Hall.

Appleby, P.G., Nolan, P.J., Gifford, D.W., Godfrey, M.J., Oldfield, F., Anderson, N.J. et al. (1986) ^{210}Pb dating by low background gamma counting. *Hydrobiologia*, 143, 21–27. Available at: https://doi.org/10.1007/BF00026640

Aufgebauer, A., Panagiotopoulos, K., Wagner, B., Schaebitz, F., Viehberg, F.A., Vogel, H. et al. (2012) Climate and environmental change in the Balkans over the last 17 ka recorded in sediments from Lake Prespa (Albania/F.Y.R. of Macedonia/Greece). *Quaternary International*, 274, 122–135. Available at: https://doi.org/10.1016/j.quaint.2012.02.015

Benjamini, Y. & Hochberg, Y. (1995) Controlling the false discovery rate: A practical and powerful approach to multiple testing. *Journal of the Royal Statistical Society Series B: Statistical Methodology*, 57(1), 289–300.

Bertrand, S., Tjallingii, R., Kylander, M. et al. (2023) Inorganic geochemistry of lake sediments: A review of analytical techniques and guidelines for interpretation. *Earth-Science Reviews*, 249, 104639. Available at: https://doi.org/10.1016/j.earscirev.2023.104639

Blomfield, F. (1805) *An essay towards a topographical history of the county Norfolk*. London: William Miller, pp. 1–39.

Boehrer, B. & Schultze, M. (2008) Stratification of lakes. *Reviews of Geophysics*, 46(2), 1–27. Available at: https://doi.org/10.1029/2006RG000210

Bouffard, D., Boegman, L., Ackerman, J.D., Valipour, R. & Rao, Y.R. (2014) Near-inertial wave driven dissolved oxygen transfer through the thermocline of a large lake. *Journal of Great Lakes Research*, 40(2), 300–307. Available at: https://doi.org/10.1016/j.jglr.2014.03.014

Bova, S., Rosenthal, Y., Liu, Z., Godad, S.P. & Yan, M. (2021) Seasonal origin of the thermal maxima at the Holocene and the last interglacial. *Nature*, 589, 548–553. Available at: https://doi.org/10.1038/s41586-020-03155-x

Boyall, L., Valcárcel, J.I., Harding, P., Hernández, A. & Martin-Puertas, C. (2023) Disentangling the environmental signals recorded in Holocene calcite varves based on modern lake observations and annual sedimentary processes in Diss Mere, England. *Journal of Paleolimnology*, 70, 39–56. Available at: https://doi.org/10.1007/s10933-023-00282-z

Brauer, A., Mangili, C., Moscariello, A. & Witt, A. (2008) Palaeoclimatic implications from micro-facies data of a 5900 varve time series from the

Piànico interglacial sediment record, southern Alps. *Palaeogeography, Palaeoclimatology, Palaeoecology*, 259(2-3), 121–135. Available at: https://doi.org/10.1016/j.palaeo.2007.10.003

Bretherton, C.S., Widmann, M., Dymnikov, V.P., Wallace, J.M. & Bladé, I. (1999) The effective number of spatial degrees of freedom of a time-varying field. *Journal of Climate*, 12(7), 1990–2009. Available at: https://doi.org/10.1175/1520-0442(1999)012<1990:TENOSD>2.0.CO;2

Bronk Ramsey, C. (2009) Bayesian analysis of radiocarbon dates. *Radiocarbon*, 51(1), 337–360. Available at: https://doi.org/10.1017/s0033822200033865

Bronk Ramsey, C. (2021) OxCal 4.4.4 calibration programme. https://c14.arch.ox.ac.uk/oxcal/OxCal.html

Cartapanis, O., Jonkers, L., Moffa-Sanchez, P., Jaccard, S.L. & de Vernal, A. (2022) Complex spatio-temporal structure of the Holocene Thermal Maximum. *Nature Communications*, 13, 5662. Available at: https://doi.org/10.1038/s41467-022-33362-1

Cohen, A.S. (2003) *Palaeolimnology: the history and evolution of lake systems*. New York: Oxford University Press. pp. 184–189.

Corella, J.P., Moreno, A., Morellón, M., Rull, V., Giralt, S., Rico, M.T. et al. (2011) Climate and human impact on a meromictic lake during the last 6,000 years (Montcortès Lake, Central Pyrenees, Spain. *Journal of Paleolimnology*, 46, 351–367. Available at: https://doi.org/10.1007/s10933-010-9443-3

Czymzik, M., Tjallingii, R., Plessen, B., Feldens, P., Theuerkauf, M., Moros, M. et al. (2023) Mid-Holocene reinforcement of North Atlantic atmospheric circulation variability from a western Baltic lake sediment record. *Climate of the Past*, 19, 233–248. Available at: https://doi.org/10.5194/cp-19-233-2023

Davies, S.J., Lamb, H.F. & Roberts, S.J. (2015) Micro-XRF Core Scanning in Palaeolimnology: Recent Developments. In: Croudace, I.W. & Rothwell, R.G., (Eds.) *Micro-XRF Studies of Sediment Cores: Applications of a Non-Destructive Tool for the Environmental Sciences, Developments in Paleoenvironmental Research*. Dordrecht: Springer Netherlands. pp. 189–226. https://doi.org/10.1007/978-94-017-9849-5_7

Davis, B.A.S., Brewer, S., Stevenson, A.C. & Guiot, J. (2003) The temperature of Europe during the Holocene reconstructed from pollen data. *Quaternary Science Reviews*, 22, 1701–1716. Available at: https://doi.org/10.1016/S0277-3791(03)00173-2

Davison, W. (1993) Iron and manganese in lakes. *Earth-Science Reviews*, 34, 119–163.

Dittrich, M. & Obst, M. (2004) Are Picoplankton Responsible for Calcite Precipitation in Lakes? *AMBIO: A Journal of the Human Environment*, 33, 559–564. Available at: https://doi.org/10.1579/0044-7447-33.8.559

Dörfler, W., Feeser, I., Hildebrandt-Radke, I. & Rzodkiewicz, M. (2022) Environment and settlement - A multiproxy record of Holocene palaeoenvironmental development from Lake Wonieść, Greater Poland. *Vegetation History and Archaeobotany*, 32, 187–204. Available at: https://doi.org/10.1007/s00334-022-00890-1

Dräger, N., Theuerkauf, M., Szeroczyńska, K., Wulf, S., Tjallingii, R., Plessen, B. et al. (2017) Varve microfacies and varve preservation record of climate change and human impact for the last 6000 years at Lake Tiefer See (NE Germany. *The Holocene*, 27, 450–464. Available at: https://doi.org/10.1177/0959683616660173

Druzhinina, O., Gedminienė, L. & van den Berghe, K. (2022) Metals in lake sediments as indicators of human activities in prehistory: Case study of the Southeastern Baltic, Kamyshovoe Lake. *Minerals*, 12(10), 1216. Available at: https://doi.org/10.3390/min12101216

Dunlea, A.G., Murray, R.W., Tada, R., Alvarez-Zarikian, C.A., Anderson, C.H., Gilli, A. et al. (2020) Intercomparison of XRF core scanning results from seven labs and approaches to practical calibration. *Geochemistry, Geophysics, Geosystems*, 21(9), e2020CG009248. Available at: https://doi.org/10.1029/2020GC009248

Engstrom, D.R., Swain, E.B. & Kingston, J.C. (2006) A palaeolimnological record of human disturbance from Harvey's Lake, Vermont: geochemistry, pigments and diatoms. *Freshwater Biology*, 15(3), 261–288.

Evans, G., Augustinus, P., Gadd, P., Zawadzki, A. & Ditchfield, A. (2019) A multi-proxy XRF inferred lake sediment record of environmental change spanning the last ca. 2230 years from Lake Kanono, Northland, New Zealand. *Quaternary Science Reviews*, 225, 106000. Available at: https://doi.org/10.1016/j.quascirev.2019.106000

Fritz, S.C. (1989) Lake Development and Limnological Response to Prehistoric and Historic Land-Use in Diss, Norfolk, U.K. *The Journal of Ecology*, 77, 182. Available at: https://doi.org/10.2307/2260924

Harding, P., Martin-Puertas, C., Sjolte, J. et al. (2022) Wind regime changes in the Euro-Atlantic region driven by Late-Holocene Grand Solar Minima. *Climate Dynamics*, 60, 1947–1961. Available at: https://doi.org/10.1007/s00382-022-06388-w

Hecky, R.E. & Kilham, P. (1988) Nutrient limitation of phytoplankton in freshwater and marine environments: A review of recent evidence on the effects of enrichment. *Limnology and Oceanography*, 22(4), 796–822. Available at: https://doi.org/10.4319/lo.1988.33.4part2.0796

Hingham, N.J. & Ryan, M.J. (2010) *The Landscape Archaeology of Anglo-Saxon England*. Boydell & Brewer.

Hyndman, R., Athanasopoulos, G., Bergmeir, C., Caceres, G. et al. 2023. forecast: Forecasting functions for timeseries and linear models. R package version 8.21.1. https://pkg.robjhyndman.com/forecast/>

Jenny, J.-P., Francus, P., Normandeau, A., Lapointe, F., Perga, M.E., Ojala, A. et al. (2016) Global spread of hypoxia in freshwater ecosystems during the last three centuries is caused by rising local human pressure. *Global Change Biology*, 22(4), 1481–1489. Available at: https://doi.org/10.1111/gcb.13193

Jones, S.E., López-Costas, O., Martínez Cortizas, A., Mighall, T.M., Stratigos, M.J. & Noble, G. (2022) Lake and crannog: A 2500-year palaeoenvironmental record of continuity and change in NE Scotland. *Quaternary Science Reviews*, 285, 107532. Available at: https://doi.org/10.1016/j.quascirev.2022.107532

Jonsson, C.E., Andersson, S., Rosqvist, G.C. & Leng, M.J. (2010) Reconstructing past atmospheric circulation changes using oxygen isotopes in lake sediments from Sweden. *Climate of the Past*, 6, 49–62. Available at: https://doi.org/10.5194/cp-6-49-2010

Jouve, G., Francus, P., Lamoureux, S., Provencher-Nolet, L., Hahn, A., Haberzettl, T. et al. (2013) Microsedimentological characterization using image analysis and μ-XRF as indicators of sedimentary processes and climate changes during Lateglacial at Laguna Potrok Aike, Santa Cruz, Argentina. *Quaternary Science Reviews*, 71, 191–204. Available at: https://doi.org/10.1016/j.quascirev.2012.06.003

Kaufman, D. (2004) Holocene thermal maximum in the western Arctic (0–180° W). *Quaternary Science Reviews*, 23, 529–560. Available at: https://doi.org/10.1016/j.quascirev.2003.09.007

Kaufman, D., McKay, N., Routson, C., Erb, M., Dätwyler, C., Sommer, P.S. et al. (2020) Holocene global mean surface temperature, a multi-method reconstruction approach. *Scientific Data*, 7(201), 201.

Keating, K.I. (1978) Blue-Green algal inhibition of diatom growth: transition from mesotrophic to eutrophic community structure. *Science*, 199(4332), 971–973.

Kelts, K. & Hsu, K.J. (1978) Freshwater carbonate sedimentation. In: Lerman, A., Ed. *Lakes: Chemistry, geology, and physics*. Springer. pp. 295–324.

Kern, O.A., Koutsodendris, A. & Mächtle, B. (2019) XRF core scanning yields reliable semiquantitative data on the elemental composition of highly organic-rich sediments: Evidence from the Füramoos peat bog (Southern Germany). Science of the Total Environment. 697. 134110. https://doi.org/10.1016/j.scitotenv.2019.134110

Liu, Z., Zhu, J., Rosenthal, Y., Zhang, X., Otto-Bliesner, B.L., Timmermann, A. et al. (2014) The Holocene temperature conundrum. *Proceedings of the National Academy of Sciences*, 111(34), 3501–3505. Available at: https://doi.org/10.1073/pnas.1407229111

Makri, S., Rey, F., Gobet, E., Gilli, A., Tinner, W. & Grosjean, M. (2020) Early human impact in a 15 000-year high-resolution hyperspectral imaging record of paleoproduction and anoxia from a varved lake in Switzerland. *Quaternary Science Reviews*, 239, 106335. Available at: https://doi.org/10.1016/j.quascirev.2020.106335

Makri, S., Wienhues, G., Bigalke, M., Gilli, A., Rey, F., Tinner, W. et al. (2021) Variations of sedimentary Fe and Mn fractions under changing lake mixing regimes, oxygenation and land surface processes during Late-glacial and Holocene times. *Science of the Total Environment*, 755(2), 143418.

Martin-Puertas, C., Brauer, A., Dulski, P. & Brademann, B. (2012) Testing climate-proxy stationarity throughout the Holocene: an example from the varved sediments of Lake Meerfelder Maar (Germany). *Quaternary Science Reviews*, 58, 56–65. Available at: https://doi.org/10.1016/j.quascirev.2012.10.023

Martin-Puertas, C., Hernandez, A., Pardo-Igúzquiza, E. et al. (2023) Dampened predictable decadal North Atlantic climate fluctuations due to ice melting. *Naure Geoscience*, 16, 357–362. Available at: https://doi.org/10.1038/s41561-023-01145-y

Martin-Puertas, C., Walsh, A.A., Blockley, S.P.E., Harding, P., Biddulph, G.E., Palmer, A. et al. (2021) The first Holocene varve chronology for the UK: Based on the integration of varve counting, radiocarbon dating and tephrostratigraphy from Diss Mere (UK). *Quaternary Geochronology*, 61, 101134. Available at: https://doi.org/10.1016/j.quageo.2020.101134

Martin-Puertas, C., Tjallingii, R., Bloemsma, M. & Brauer, A. (2017) Varved sediment responses to early Holocene climate and environmental changes in Lake Meerfelder Maar (Germany) obtained from multivariate analyses of micro X-ray fluorescence core scanning data. *Journal of Quaternary Science*, 32, 427–436. Available at: https://doi.org/10.1002/jqs.2935

Mayes, J. (2000) Changing regional climatic gradients in the United Kingdom. *The Geographical Journal*, 166(2), 125–138. Available at: https://doi.org/10.1111/j.1475-4959.2000.tb00013.x

Müller, D., Tjallingii, R., Płóciennik, M., Luoto, T.P., Kotrys, B., Plessen, B. et al. (2021) New insights into lake responses to rapid climate change: the Younger Dryas in Lake Gościąż, central Poland. *Boreas*, 50, 535–555. Available at: https://doi.org/10.1111/bor.12499

Naeher, S., Gilli, A., North, R.P., Hamann, Y. & Schubert, C.J. (2013) Tracing bottom water oxygenation with sedimentary Mn/Fe ratios in Lake Zurich, Switzerland. *Chemical Geology*, 352, 125–133.

Needham, S. (2007) 800 BC, the great divide, in: The Earlier Iron Age in Britain and the Near Continent.

Olsen, J., Björck, S., Leng, M.J., Gudmundsdóttir, E.R., Odgaard, B.V., Lutz, C.M. et al. (2010) Lacustrine evidence of Holocene environmental change from three Faroese lakes: a multiproxy XRF and stable isotope study. *Quaternary Science Reviews*, 29, 2764–2780. Available at: https://doi.org/10.1016/j.quascirev.2010.06.029

Osman, M.B., Tierney, J.E., Zhu, J., Tardif, R., Hakim, G.J., King, J. et al. (2021) Globally resolved surface temperatures since the Last Glacial Maximum. *Nature*, 599, 239–244. Available at: https://doi.org/10.1038/s41586-021-03984-4

Peglar, S.M. (1993) The development of the cultural landscape around Diss Mere, Norfolk, UK, during the past 7000 years. *Review of Palaeobotany and Palynology*, 76, 1–47. Available at: https://doi.org/10.1016/0034-6667(93)90079-A

Peglar, S.M., Fritz, S.C. et al. (1984) Composition and formation of laminated sediments in Diss Mere, Norfolk, England. Boreas.

Peglar, S.M., Fritz, S.C. & Birks, H.J.B. (1989) Vegetation and land-use history at Diss, Norfolk, U.K. *The Journal of Ecology*, 77, 203–222. Available at: https://doi.org/10.2307/2260925

Peti, L. & Augustinus, P.C. (2022) Micro-XRF-inferred depositional history of the Orakei maar lake sediment sequence, Auckland, New Zealand. *Journal of Paleolimnology*, 67, 327–344. Available at: https://doi.org/10.1007/s10933-022-00235-y

Pleskot, K., Tjallingii, R., Makohonienko, M., Nowaczyk, N. & Szczuciński, W. (2018) Holocene paleohydrological reconstruction of Lake Strzeszyńskie (western Poland) and its implications for the central European climatic transition zone. *Journal of Paleolimnology*, 59, 443–459. Available at: https://doi.org/10.1007/s10933-017-9999-2

Plummer, L.N. & Busenberg, E. (1982) The solubilities of calcite, aragonite and vaterite in CO_2-H_2O solutions between 0 and 90 C, and an evaluation of the aqueous model for the system $CaCO_3$-CO_2-H_2O. *Geochimica et Cosmochimica Acta*, 46(6), 1011–1040. Available at: https://doi.org/10.1016/0016-7037(82)90056-4

Pursehouse, E. 1961. Hemp: a forgotten Norfolk crop. Eastern Daily Press. 25.

R Core Team. 2023. R: A language and Environment for Statistical Computing. R Foundation for Satistical Compluting, Vienna, Austria. https://www.R-project.org

Rasmussen, S.O., Andersen, K.K., Svensson, A.M. et al. (2006) A new Greenland ice core chronology for the last glacial termination. *Journal of Geophysical Research: Atmospheres*, 111. Available at: https://doi.org/10.1029/2005JD006079

Reimer, P.J., Austin, W.E.N., Bard, E., Bayliss, A., Blackwell, P.G., Bronk Ramsey, C. et al. (2020) The IntCal20 Northern Hemisphere Radiocarbon Age Calibration Curve (0–55 cal kBP). *Radiocarbon*, 62, 725–757.

Reynolds, S. (1985) What Do We Mean by "Anglo-Saxon" and "Anglo-Saxons"? *The Journal of British Studies*, 24, 395–414. Available at: https://doi.org/10.1086/385844

Roeser, P., Dräger, N., Brykała, D., Ott, F., Pinkerneil, S., Gierszewski, P. et al. (2021) Advances in understanding calcite varve formation: new insights from a dual lake monitoring approach in the southern Baltic lowlands. *Boreas*, 50, 419–440. Available at: https://doi.org/10.1111/bor.12506

Rull, V., Vegas-Vilarrúbia, T., Corella, J.P. & Valero-Garcés, B. (2021) Bronze Age to Medieval vegetation dynamics and landscape anthropization in the southern-central Pyrenees. *Palaeogeography, Palaeoclimatology, Palaeoecology*, 571, 110392. Available at: https://doi.org/10.1016/j.palaeo.2021.110392

Ryther, J.H. & Officer, C.B. (1981) Impact of nutrient enrichment on water uses. in Contemporary issues in science and society.

Tardif, R., Hakim, G.J., Perkins, W.A., Horlick, K.A., Erb, M.P., Emile-Geay, J. et al. (2019) Last Millennium Reanalysis with an expanded proxy database and seasonal proxy modeling. *Climate of the Past*, 15, 1251–1273. Available at: https://doi.org/10.5194/cp-15-1251-2019

Tjallingii, R., Röhl, U., Kölling, M. et al. (2007) Influence of the water content on X-ray fluorescence core-scanning measurements in soft marine sediments. *Geochemistry, Geophysics, Geosystems*, 8. Available at: https://doi.org/10.1029/2006GC001393

Waller, M.P. & Schofield, J.E. (2007) Mid to late Holocene vegetation and land use history in the Weald of south-eastern England: multiple pollen profiles from the Rye area. *Vegetation History and Archaeobotany*, 16, 367–384.

Walsh, A.A., Blockley, S.P.E., Milner, A.M. & Martin-Puertas, C. (2023) Updated age constraints on key tephra markers for NW Europe based on a high-precision varve lake chronology. *Quaternary Science Reviews*, 300, 107897. Available at: https://doi.org/10.1016/j.quascirev.2022.107897

Walsh, A.A., Blockley, S.P.E., Milner, A.M., Matthews, I.P. & Martin-Puertas, C. (2021) Complexities in European Holocene cryptotephra dispersal revealed in the annually laminated lake record of Diss Mere, East Anglia. *Quaternary Geochronology*, 66, 101213. Available at: https://doi.org/10.1016/j.quageo.2021.101213

Warden, L., Moros, M., Neumann, T., Shennan, S., Timpson, A., Manning, K. et al. (2017) Climate induced human demographic and cultural change in northern Europe during the mid-Holocene. *Scientific Reports*, 7, 15251. Available at: https://doi.org/10.1038/s41598-017-14353-5

Weltje, G.J., Bloemsma, M.R., Tjallingii, R. et al. (2015) Prediction of Geochemical Composition from XRF Core Scanner Data: A New Multivariate Approach Including Automatic Selection of Calibration Samples and Quantification of Uncertainties. in: Croudace, I.W., Rothwell, R.G., (Eds.) *Micro-XRF Studies of Sediment Cores: Applications of a Non-Destructive Tool for the Environmental Sciences, Developments in Paleoenvironmental Research*. Springer Netherlands: Dordrecht. pp. 507–534. https://doi.org/10.1007/978-94-017-9849-5_21

Weltje, G.J. & Tjallingii, R. (2008) Calibration of XRF core scanners for quantitative geochemical logging of sediment cores: Theory and application. *Earth and Planetary Science Letters*, 274, 423–438. Available at: https://doi.org/10.1016/j.epsl.2008.07.054

Yang, H. (2010) Historical mercury contamination in sediments and catchment soils of Diss Mere, UK. *Environmental Pollution*, 158, 2504–2510. Available at: https://doi.org/10.1016/j.envpol.2010.03.015

Yeloff, D., van Geel, B., Broekens, P., Bakker, J. & Mauquoy, D. (2007) Mid- to late-Holocene vegetation and land-use history in the Hadrian's Wall region of northern England: the record from Butterburn Flow. *The Holocene*, 17, 527–538. Available at: https://doi.org/10.1177/0959683607076472

Zander, P.D., Żarczyński, M., Tylmann, W., Rainford, S. & Grosjean, M. (2021) Seasonal climate signals preserved in biochemical varves:

insights from novel high-resolution sediment scanning techniques. *Climate of the past*, 17, 2055–2071. Available at: https://doi.org/10.5194/cp-17-2055-2021

Zolitschka, B., Francus, P., Ojala, A.E.K. & Schimmelmann, A. (2015) Varves in lake sediments - A review. *Quaternary Science Reviews*, 117, 1–41. Available at: https://doi.org/10.1016/j.quascirev.2015.03.019

Żarczyński, M., Wacnik, A. & Tylmann, W. (2019) Tracing lake mixing and oxygenation regime using the Fe/Mn ratio in varved sediments: 2000 year-long record of human-induced changes from Lake Żabińskie (NE Poland). *Science of the Total Environment*, 657, 585–596. Available at: https://doi.org/10.1016/j.scitotenv.2018.12.078